

Acoustic Emission During Slow Crack Growth (2nd paper)

Osam SANO*, Shoji OGINO* and Yoshiaki MIZUTA*
(Received July 15, 1981)

Abstract

Double torsion testing was carried out for seven specimens of Oshima granite and Murata basalt. About 200 acoustic emissions for each rock were monitored and their wave forms were stored digitally by a transient event recorder. Fourier analysis was carried out for the first motion of each acoustic emission.

In log-log plots, the relation between the power spectrum and the frequency could be regarded as two straight lines and the corner frequency was determined by the intersection of these lines. Acoustic emissions having high corner frequency had the lower maximum power spectrum. The maximum power spectrum increased with increasing stress intensity factor at the tip of the macrocrack. The corner frequency, in contrast, decreased with increasing stress intensity factor.

Introduction

When rock is subject to a deviatoric stress, many microcrackings occur prior to the macroscopic fracture. These microcrackings emit elastic radiations known as elastic shocks or acoustic emissions. A monitoring of acoustic emissions is a useful tool for the detection of microcrackings within rock in laboratory, and has a possibility of a location of the highly stressed region in situ. Acoustic emission studies in rock mechanics have been carried out by various authors from different viewpoints.

Associated with slow crack growth, acoustic emissions were observed for porcelain¹⁾, granite and gabbro²⁾, and granite and basalt³⁾. However, no or little acoustic emissions could be observed for quartz⁴⁾, and marble and tuff⁵⁾. When the acoustic emission can be detected, the emission rate has a close relation with the growth rate of the macrocrack^{1), 2), 3)}. Sano⁶⁾ showed that the epicenter of the emission event lies in the proximity of the curved front region of the macrocrack. And hence, it seems to be natural that the microcracking emitting acoustic radiation leads the growth of the macrocrack. However, Sano⁶⁾ also suggested that the emission events were concomitant with the macrocrack and could not manily control the growth of the macrocrack. The analysis of the acoustic emissions will potentially provide a clue to the interpretation of the physical mechanisms of the slow crack growth.

In the first paper³⁾, we showed that the dominant frequency of the acoustic emissions ranged from 100 kHz to 1 MHz, and decreased with increasing K_I or with increasing crack growth rate. However, the number of data in their measurement were so small (70 events) that the scatterings of data concealed any indication of the change in ampli-

* Department Mining and Mineral Engineering

tude of the acoustic emissions with increasing K_I . In this paper, Fourier spectral analyses of about 200 events for each rock was carried out in order to clarify the spectral change with increasing K_I by using double torsion method.

Experimental technique

Double torsion equipment was described in detail in previous paper³⁾. Load was applied by a dead load. Rocks studied was Murata basalt and Oshima granite whose physical properties are listed in Table 1. The specimens were cut parallel to each other by a diamond saw and then ground flat and parallel by a lathe. Each specimen was 4 cm wide \times 2.5 mm thick \times 10 cm long. A guiding groove was precut to 1 mm in width and 0.5 mm in depth.

Table 1 Physical properties of Murata basalt and Oshima granite

Rock type	Young's modulus	Poisson's ratio
Murata basalt	72.4 GPa	0.24
Oshima granite	60.9	0.28

Each run was carried out under constant load which was raised incrementally. The mode I stress intensity factor, K_I , at the crack-tip was calculated according to Williams and Evans⁷⁾, namely

$$K_I = PW_m \left(\frac{3(1+\nu)}{W d n d^3} \right)^{\frac{1}{2}}, \quad (1)$$

Where P is a total load, W is the width of the specimen, W_m is the moment arm, d is the specimen's thickness, d_n is the plate thickness at the crack plane and ν is the Poisson's ratio. The growth rate of the crack corresponding to K_I was estimated from K_I -V diagram described in previous paper³⁾.

Acoustic emissions were detected by plumbum-titanate-plumbum-zirconate disks which were resonant at 5 MHz. Amplification was achieved by a differential pre-amplifier which had a 46 dB gain and input impedance of 120 k Ω . The overall frequency response of the amplification was flat from 10 kHz to 3 MHz.

The signals of the emission events randomly sampled were stored digitally by a transient event recorder which had a memory length of 1024 words and a digitized interval varying from 50 ns to 1 s. In this experiment, the sampling interval was fixed at 50 ns/word. Analyses by fast Fourier transform were carried out by a desk-top computer connected with the transient event recorder through the IEEE-488 interface bus.

Results and discussion

Typical examples of the results on the Fourier analyses of first motion of the acoustic emissions are shown in Fig. 1 where data are plotted on double logarithmic coordinates.

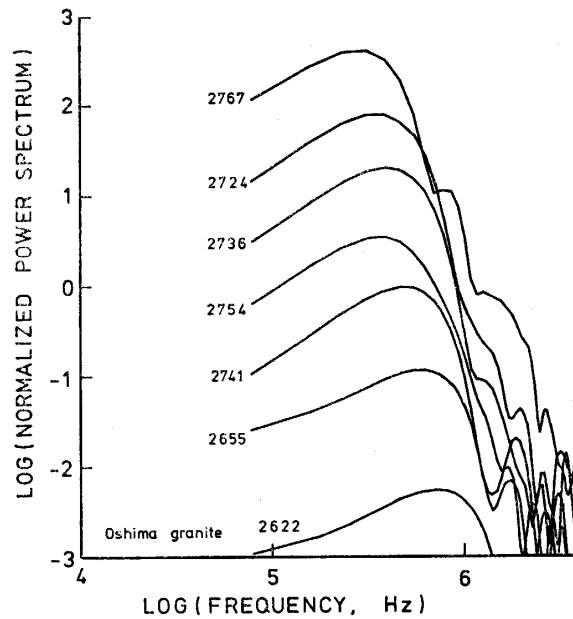


Fig. 1 Typical examples of the power spectra of the acoustic emissions observed on Oshima granite. Data are plotted on double logarithmic coordinates. AE numbers are indicated.

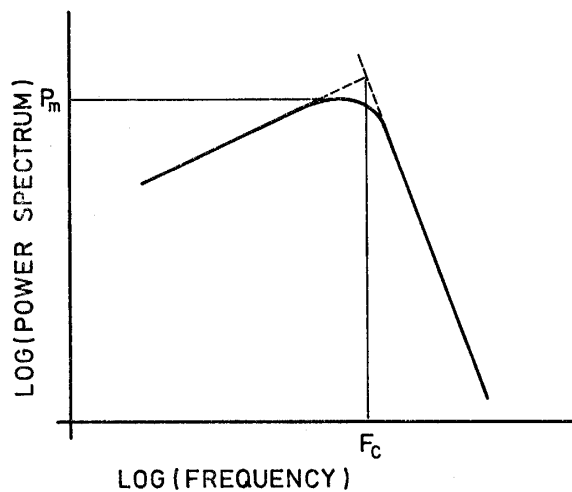


Fig. 2 Idealized power spectrum. The data can be approximated by two straight lines. The corner frequency is defined by the intersection of these lines.

Also for the thin plate, the velocity of the dilatational wave is the fastest of all other modes, and the results exhibit the characteristics of the longitudinal wave components of the acoustic emissions. Each spectrum shown in Fig. 1 can be approximated by two straight lines as schematically shown in Fig. 2. A corner frequency, F_c , is defined by an intersection of these two straight lines.

In figures 3 and 4, the maximum power spectrum is plotted against the corner

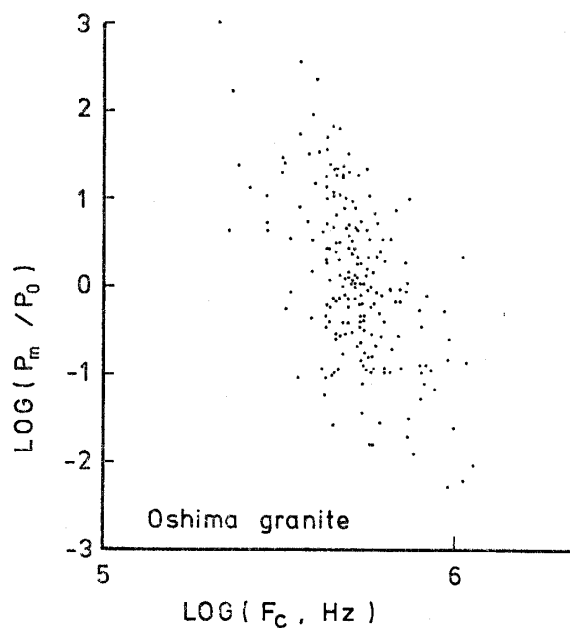


Fig. 3 The maximum power spectrum versus corner frequency observed on Oshima granite. A clear tendency that the higher the corner frequency, the lower the maximum power spectrum can be seen.

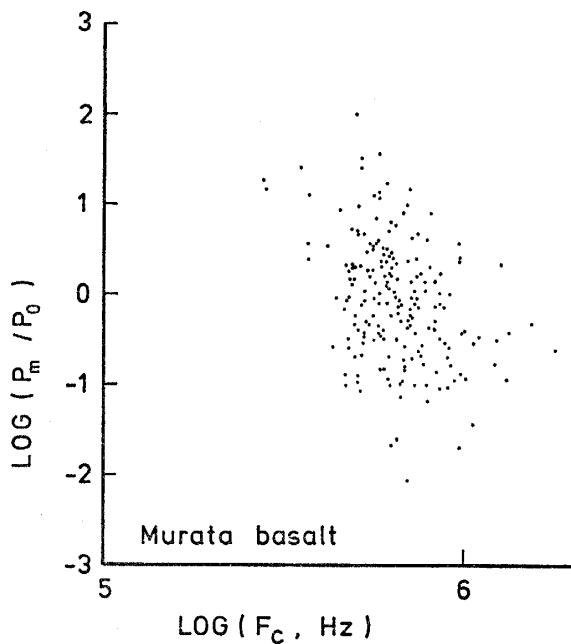


Fig. 4 The maximum power spectrum versus corner frequency observed on Murata basalt. The same tendency as in Fig. 3 can be seen.

frequency on double logarithmic coordinates. In these figures as well as in Fig. 1, we can see clearly the tendency that the higher the maximum power spectrum, the lower

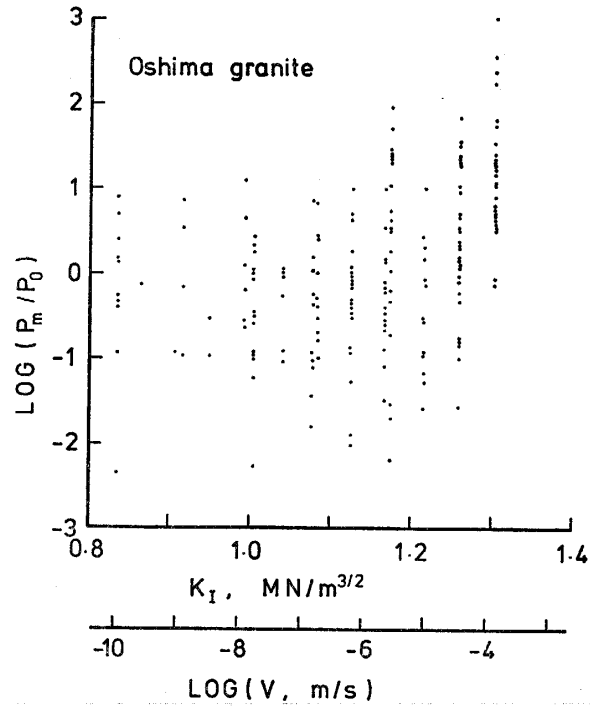


Fig. 5 Relationship between the maximum power spectrum and the stress intensity factor or the growth rate of the macrocrack. The maximum power spectrum increased with increasing K_I .

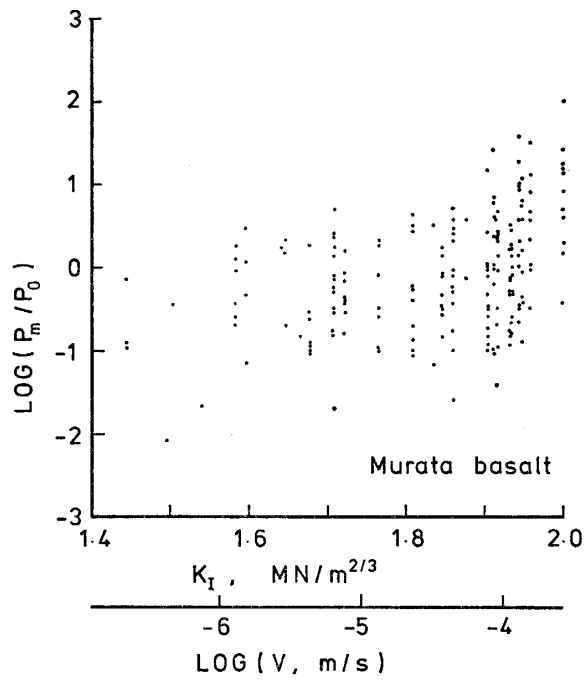


Fig. 6 The same as in Fig. 5.

the corner frequency. For both rocks, the corner frequency of the acoustic emissions ranged from 100 kHz to 2 MHz, which obviously corresponds with the previous observations^{3),8)} that the dominant frequency of acoustic emissions ranged from 100 kHz to 1 MHz.

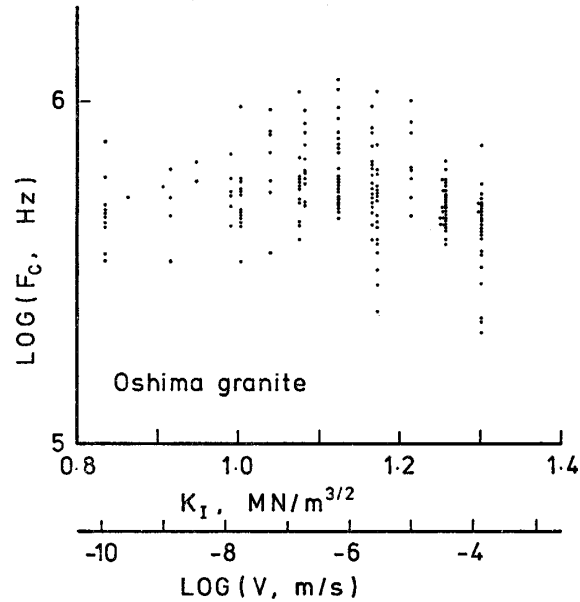


Fig. 7 Corner frequency as a function of K_I or V . The corner frequency decreased with increasing K_I or with increasing V .

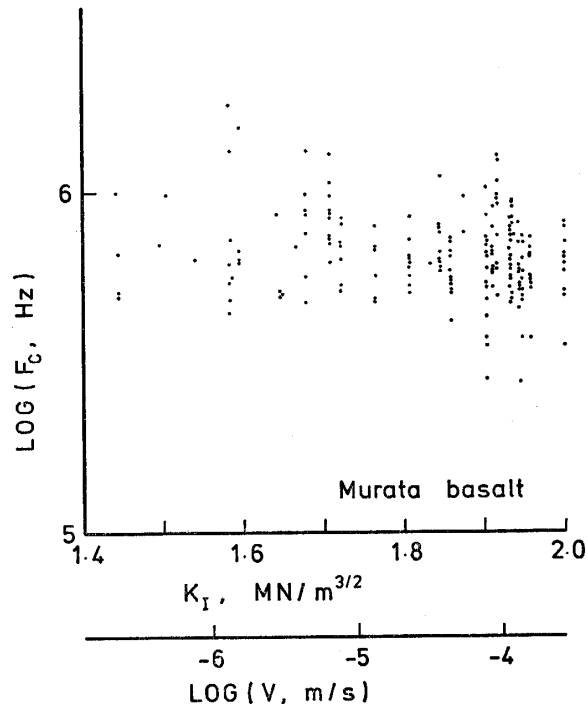


Fig. 8 The same as in Fig. 7.

In figures 5 and 6, the maximum power spectrum is plotted as a function of the mode I stress intensity factor, K_I , at which the acoustic emission was observed. In these figures, a clear tendency that the maximum power spectrum increased with increasing K_I or with increasing crack velocity of the macrocrack. The lower limit of the maximum power spectrum in these figures has not any physical significance, for it is responsible to a threshold level and an input range of the transient event recorder.

Figures 7 and 8 show the relationship between the corner frequency, F_C , and K_I as well as the crack growth rate, V . Because the lower limit of the maximum power spectrum shown in Figs. 5 and 6 has little physical significance, and because the corner frequency tends to higher with decreasing the maximum power spectrum as shown in Fig. 1, 3 and 4, the upper limit shown in Figs. 7 and 8 has also little physical significance. However, the lower limit in F_C - K_I relation shows a tendency that the corner frequency decreased with increasing K_I or with increasing growth rate of the macrocrack.

Sano⁶⁾ showed that the epicenter of the emission event lies on the proximity of the macrocrack, and hence physical properties of the propagation path of the acoustic emission should not have changed associated with microcrackings. So, the changes in amplitude and in corner frequency should be responsible to the changes in emission events themselves.

The energy release, E , associated with the microcracking can be expressed by

$$E = k_1 \sigma^2 v, \quad (2)$$

where σ is the stress drop, v is the fracturing volume of microcracking and k_1 is a constant. The amplitude of the first motion, a , can be, as a first approximation, expressed by

$$E = k_2 a^\gamma, \quad (3)$$

where k_2 is a constant and γ is also a constant ranging from 1.5 to 2. If the stress drop and/or the size of the emission event increased with increasing K_I or with increasing crack velocity, V , the spectral amplitude of the acoustic emission will increase.

Because the stress drop can be proportional to the local tensile stress around the tip of the macrocrack and the local stress can be represented by K_I , the stress drop, σ , can be exchanged for K_I . Combining equations (2) and (3), we obtain

$$a = k_3 K_I^{\frac{2}{\gamma}} V^{\frac{1}{\gamma}}, \quad (4)$$

where k_3 is a constant. The equation (4) suggests that the amplitude should increase by, at most, only twice, when the stress intensity factor increases from the left hand side end to the right hand side end of figures 5 and 6. However, the maximum power spectrum increased further. And hence, the increase in the maximum power spectrum with increasing K_I or with increasing crack velocity is responsible not only to the increase in the stress drop but also to the increase in the fracturing volume. The increase in the size of the microcracking will tend to decrease the corner frequency as shown in Figs. 7 and 8.

In the statistical analysis of the acoustic emissions, the cumulative number of acoustic

emissions are usually plotted against the maximum amplitude on double logarithmic coordinates. The data are generally regarded as a straight line in log-log plots. The slope of the straight line is called b-value. Atkinson and Rawlings⁹⁾ showed that the b-value decreased with increasing K_I . Their results agree well with present observation that the maximum power spectrum increased with increasing K_I .

Acknowledgements

The authors are grateful to K.Kubo and K.Fukushima for the assistance in the experiments.

References

- 1) Evans, A.G. and M. Linzer, Failure prediction in structural ceramics using acoustic emission, *J. Amer. Ceram. Soc.*, **56**, 575-581 (1973).
- 2) Atkinson, B.K. and R. D. Rawlings, Acoustic emission during subcritical tensile cracking of gabbro and granite, *Eos*, **60**, 740 (1979).
- 3) Sano, O. and S. OginO, Acoustic emission during slow crack growth (1st paper), *Tech. Rep. Yamaguchi Univ.*, **2**, 381-388 (1980).
- 4) Martin, R. J., III and W. B. Durham, Mechanism of crack growth in quartz, *J. Geophys. Res.*, **90**, 4837-4844 (1975).
- 5) Egami, S., Personal communications.
- 6) Sano, O., A note on the sources of acoustic emissions associated with subcritical crack growth, *Int. J. Rock Mech. Min. Sci. & Geomech. Abstr.*, **18**, 259-263 (1981).
- 7) Williams, D. P. and A. G. Evans, A simple method for studying slow crack growth, *J. Test. Eval.*, **1**, 264-270 (1972).
- 8) Scholz, C. H., Microfracturing and the inelastic deformation of rock in compression, *J. Geophys. Res.*, **73**, 1417-1432 (1968).
- 9) Atkinson, B. K. and R. D. Rawlings, Acoustic emission during stress corrosion cracking in rocks, *Proc. 3rd Ewing Symp. on Earthquake prediction* (1981) [in press].